CLASP (Continuous lifestyle awareness through sweat platform): A novel sensor for simultaneous detection of alcohol and glucose from passive perspired sweat

Ashlesha Bhide[a], Sriram Muthukumar[b], and Shalini Prasad[a,*]

[a]Department of Bioengineering, University of Texas at Dallas, 800 West Campbell Road, Richardson, TX 75080, USA

[b]Enlisense LLC, 1813 Audubon Pond way, Allen, TX 75013, USA

Abstract

Wearable- IOT based low- cost platforms can enable dynamic lifestyle monitoring through enabling promising and exciting opportunities for wellness and chronic- disease management in personalized environments. Diabetic and pre- diabetic populations can modulate their alcohol intake by tracking their glycemic content continuously to prevent health risks through these platforms. We demonstrate the first technological proof of a combinatorial biosensor for continuous, dynamic monitoring of alcohol and glucose in ultra- low volumes (1– 5μL) of passive perspired sweat towards developing a wearable- IOT based platform. Non-invasive biosensing in sweat is achieved by a unique gold- zinc oxide (ZnO) thin film electrode stack fabricated on a flexible substrate suitable for wearable applications. The active ZnO sensing region is immobilized with enzyme complexes specific for the detection of alcohol and glucose through non- faradaic electrochemical impedance spectroscopy (EIS) and chronoamperometry (CA). Biomolecular interactions occurring at the electrode- sweat interface are represented by the impedance and capacitive current changes in response to charge modulations arising in the double layer. We also report the detection of alcohol concentrations of 0.01– 100 mg/dl and glucose concentrations of 0.01– 50 mg/dl present in synthetic sweat and perspired human sweat. The limit of detection obtained for alcohol and glucose was found to be 0.1 mg/dl in perspired human sweat. Cross-reactivity studies revealed that glucose and alcohol did not show any signal response to cross-reactive molecules. Furthermore, the stable temporal response of the combinatorial biosensor on continuous exposure to passive perspired human sweat spiked with alcohol and glucose over a 120-minute duration was demonstrated.

*Corresponding author. shalini.prasad@utdallas.edu.

1. Introduction

Internet of things (IOT) platforms have emerged as a class of rapidly evolving embedded technologies that interconnects everyday objects in the environment with sensors using internet to create application- specific solutions for remote, real- time monitoring (Haghi et al., 2017) (S. Hiremath et al., 2014). IOT has primarily made its way into the biosensing applications market through continuous self- tracking of health indicators and preventive medicine to provide for immediate care without the need of hospitalization (Swan, 2012). Rise in health risks and the steep increase in medical costs associated with treatments has led to the transformation of the current health care system into a highly industrialized ecosystem through the emergence of wearable personal devices. In addition to wellness management, wearable biosensing technology offers low- cost diagnostic solutions for chronic and fatal disease management in remote locations. (PwC, 2014). By 2021, healthcare devices will dominate the IOT space and is expected to grow into $45.4 billion market by then (Evans, 2011). Wearable sensors provide users with the opportunity of seamless monitoring of the body's vital parameters and disease symptoms in a time controlled manner. With wellness devices gaining traction, one of the daunting challenges being faced in healthcare is the need for continuous, dynamic non-invasive monitoring of biochemical markers to understand chronic health conditions. Hence, integration of wearable diagnosis devices on an IOT platform proves promising for enabling continuous, point- of- care chronic disease detection improving early stage detections and providing the user with warnings to seek medical care. Existing wearables devices monitor digital biomarkers to track heart rate and physical activity, however, there is no information obtained on human health status which can be understood by probing biochemical markers. Recent advances have been made towards understanding easily accessible human biofluids (sweat, saliva, urine) to non-invasively monitor biomarkers that reflect the physiological state of the body. Perspired human sweat is recognized to be a highly attractive source of valuable information for this type of monitoring, and due to its ease of access, presence of biomarkers, stimulation, collection, and analysis (Jason, 2016). Literature studies show clinical correlations between sweat analyte and blood analyte levels which confirm that there is value in investigating sweat of wellness and disease management (Moyer et al., 2012) (Gamella et al., 2014). Portable bioelectronic devices capable of detecting electrolytes, glucose, and lactate in small-volumes of sweat using amperometric techniques have been demonstrated previously (Azevedo et al., 2005) (Gao et al., 2016) (Anastasova et al., 2017) (Jia et al., 2013) (Thomas et al., 2012) (Abrar et al., 2016). Alcohol and glucose are two biochemical markers that have a significant impact on human lifestyle. Alcohol consumption by diabetics and pre- diabetics can alter blood sugar levels to either hyperglycemic or hypoglycemic stages depending on their nourishment state (Emanuele et al., 1998). In the 18– 50 age group of the U.S., an estimated population of 3 billion are diagnosed with diabetes and 27. 4 billion are prediabetic (Diabetes.org, 2017). Almost 37% of the total U.S. population consumes alcohol

at moderate levels (NIAAA, 2015). A curvilinear relationship exists between alcohol consumption and incidence of type 2 diabetes (Babor et al., 2012) posing serious risks to a large demographic within this age group. Hence, there is an imminent need to monitor the effects of alcohol consumption on blood glucose levels for health and lifestyle management. Passive sweat based dynamic monitoring of these two biochemical markers offers a paradigm shifting opportunity towards wholistic on-body monitoring.

In this work, we have effectively demonstrated for the first time a wholistic approach towards biosensing alcohol and glucose combinatorially in a continuous, dynamic manner in ultra- low volumes (1– 5μL) of passive perspired human sweat. We also report the robust and stable performance of the combinatorial biosensor in perspired human sweat and synthetic sweat (SS) buffers of varying pH ranges 4– 8. We observed that pH changes in sweat microenvironment does not influence the performance of the developed biosensor enabling the continuous operation of the sensor without degradation in sensor response. AC- based EIS and DC- based CA techniques are the two detection modalities used to report the impedance and current changes in response to the target concentrations presented to biosensing system. EIS and CA provides an insight into the biomolecular interactions occurring at the electrode- buffer interface through which information regarding the target analyte concentrations can be extracted (Bard and Faulkner, 2000) (Scholz, 2015). Futhermore, the selectivity and the specificity of the combinatorial biosensor towards target analytes has been validated to demonstrate the feasibility of detection in human sweat buffer. Dynamic responses to varying levels of the biomolecules was demonstrated for a period of ~120 minutes.

2. Materials and Methods

2.1 Materials and reagents

Polyamide substrates (pore size – 200nm, thickness – 60μm) were obtained from GE Healthcare Life Sciences (Piscataway, NJ, USA). The linker molecule dithiobis succinimidyl propionate (DSP), dimethyl sulfoxide (DMSO), and 1X phosphate buffered saline (PBS) were purchased from Thermo Fisher Scientific Inc. (Waltham, MA, USA). Salt-free streptavidin from Streptomyces avidiini (13 units/mg protein), alcohol oxidase enzyme from Pichia pastoris (10–40 units/mg protein), glucose oxidase from Asperigillus niger (100,000–250,000 units/g), D-(+)- glucose, absolute ethyl alcohol (99.5%) were purchased from Sigma- Aldrich (St. Louis, MO, USA). Long arm NHS- biotin was purchased from Vector laboratories (Burlingame, CA, USA). Glucose oxidase antibody was obtained from Abcam (Cambridge, MA, USA). Glucose oxidase antibody was diluted in 1X PBS. Streptavidin was lyophilized in 1X PBS and biotin was dissolved in DMSO. Alcohol oxidase enzyme was biotinylated using the protocol stated in Du *et. al* (Du et al., 1996). Synthetic sweat was prepared as per the recipe described in M.T. Mathew *et. al* (Mathew et al., 2008). The pH range was varied by varying the concentrations of the constituents. Single donor human sweat of pH ~6 was purchased from Lee Biosolutions Inc. (Maryland Heights, MO, USA). No preservatives were added to this product and it was stored at −20°C.

2.2 Sensor fabrication

The combinatorial biosensing stack deposited on flexible nanoporous polyamide substrate is shown in Fig 1A. The biosensing stack comprises of gold electrodes and a ZnO active sensing region. The details on fabrication of the electrode stack have been outlined in the previous work (Munje et al., 2017).

2.3 Sensor calibration in synthetic sweat and perspired human sweat for alcohol detection

The immunoassay developed on the combinatorial biosensor towards detection of alcohol in SS and human sweat buffers is shown in Fig. 1B. The biosensor was functionalized with 10mM DSP thiol- cross linker diluted in dimethylsulfoxide (DMSO) by dispensing on the ZnO sensing region for 3 hours in dark. A sample volume of 3μL is utilized throughout the experimentation. Sample solutions were dispensed on the side behind the electrode fabricated region of the sensor. The immunoassay for alcohol detection was carried out as outlined in Du *et. al* (Du et al., 1996). SS solution was dispensed on the sensing region depending on the detection buffer. This step was the baseline measurement for computing impedance changes. Pure alcohol was diluted in SS buffers in logarithmically increasing concentration range between 0.01– 100 mg/dl. Alcohol dilutions in sweat were dispensed on the sensor in increasing dose concentrations and incubated for 10 minutes each. EIS and CA measurements were performed after every immobilization step. Single frequency EIS measurements recorded the impedance measurements over 5 minutes and were taken using a potentiostat (Gamry Instruments, Warminster, PA, USA) after applying an AC excitation signal of $10mV_{rms}$ at 100Hz frequency. CA measurements were carried out using the same potentiostat after applying a constant step voltage of ~0.6 V for 1 minute (Kim et al., 2016) . Similar protocols as followed for detection of alcohol in in human sweat. All data is represented as mean± standard error of mean (SEM).

The calibration dose responses (CDR) for synthetic and human sweat buffers obtained using EIS and CA were calculated for n= 3 replicates. The combinatorial biosensor's EIS response is represented as the percentage change in impedance between the baseline step and the dose concentration step. The percentage change in impedance is the change in impedance observed in response to the target biomolecule concentration with respect to the baseline in the absence of target biomolecule [see Supplementary information]. The limit of detection (LOD) is the smallest concentration of target biomolecules that is reliably detected beyond the specific signal threshold (SST). The chronoamperometric CDRs obtained in synthetic and human sweat buffers are plotted in terms of change in average steady state current of the dose concentration step with respect to the average steady state current obtained for the baseline measurement step. SST for CDR's obtained using both the techniques are computed using a signal to noise ratio (SNR) of 3 [see Supplementary information] (Armbruster and Pry, 2008).

2.4 Sensor calibration in synthetic sweat and perspired human sweat for glucose detection

The glucose detection immunoassay as shown in Fig. 1B developed on the combinatorial biosensor was adapted based on the protocol described in Munje et. al. (Munje et al., 2017) .

Glucose dilutions of concentrations from 0.01– 50 mg/dl were made in SS and human sweat buffer solutions. The calibration dose responses using EIS and CA techniques were obtained for n= 3 replicates. The computed sensor metrics for calibration in synthetic and human sweat for alcohol and glucose detection are shown in Tables S1– S4.

2.5 Evaluation of cross reactivity on alcohol and glucose biosensors with interferents in synthetic sweat of pH 6

The specificity of the combinatorial biosensing system was tested through the sensor's crossreactivity of glucose biomolecules on the alcohol sensor and alcohol biomolecules on the glucose sensor. All alcohol and glucose dilutions were made in SS pH 6. Cross reactivity studies were performed for n= 3 replicates by dispensing varying glucose concentrations in the range 0.01–100 mg/dl on the alcohol biosensor and by dispensing alcohol concentrations varying from 0.01–50 mg/dl on the glucose biosensor. Percentage change in impedance captured are computed at 100Hz.

2.6 Continuous monitoring of alcohol in perspired human sweat

Continuous, dynamic monitoring of alcohol in perspired human sweat was performed by dispensing 3μL of sweat alcohol dose concentrations in the range 3– 125 mg/dl (≈ <1– 3 drinks) for 9 minutes on the ZnO sensing region in succession over a 110 minutes duration. Alcohol concentrations of 1 mg/dl and 10 mg/dl were prepared by spiking alcohol in human sweat. 1mg/dl alcohol dose was dispensed on the sensing region three times followed by nine doses of 10 mg/dl alcohol concentration in progression to simulate the ingestion of <1– 3 standard drinks. The dynamic impedance response of the biosensing system for continuous sweat alcohol monitoring was measured at 100Hz.

2.7 Continuous, dynamic monitoring of the effect of hypoglycemic and hyperglycemic glucose levels on perspired human sweat alcohol content

The effect of hypoglycemic glucose levels on sweat alcohol content was monitored in a continuous manner over a 120 minutes window by dispensing 3μL solution of glucose and alcohol cocktail spiked in human sweat onto the ZnO sensing region functionalized with alcohol detection immunoassay. Two cocktail solutions consisting of hypoglycemic and hyperglycemic glucose concentrations with alcohol concentrations equivalent to <1–3 drinks as shown in Fig. 6B were made. These solutions were dispensed every 9 minutes on the biosensing region in progression and the dynamic impedance response was measured at 100Hz.

2.8 Continuous, dynamic monitoring of perspired sweat glucose on consumption of <1–2 standard drinks

The effect of consuming alcohol equivalent to <1– 3 drinks on the sweat glucose content was continuously monitored over a period of 120 minutes. Cocktail solutions were prepared by spiking glucose and alcohol cocktail made in human sweat buffer solution in combinations as shown in Fig. 6B. The cocktail combinations were dispensed every 9 minutes in progression on the biosensing region functionalized with glucose detection

immunoassay in 3μL volume. Individual dynamic impedance responses were obtained at 100Hz for glucose levels combined with alcohol concentration equivalent to <1–3 drinks.

3. Results and discussion

3.1 Modulation of hybrid electrode- solution interface to evaluate the sweat- based combinatorial biosensor's performance through EIS and CA techniques

The combinatorial biosensor, as shown in Fig. 1A, that was designed for the detection of alcohol and glucose employs a novel hybrid electrode with gold as the measurement electrode and a thin film of zinc oxide (ZnO) as the active sensing region on a flexible nanoporous substrate. The active sensing region of the biosensor is surface functionalized with specific enzyme biomolecule complexes for alcohol and glucose detection as shown in Fig. 1B. The response of the functionalized biosensor to the biomolecules of interest is captured through EIS and CA techniques (Daniels and Pourmand, 2007). The response of the combinatorial biosensor to the varying dose concentrations of the target biomolecule can be understood through non-faradaic electrochemical impedance spectroscopy (EIS). Non-faradaic EIS is a label- free, AC technique wherein a low amplitude sinusoidal excitation voltage over a wide frequency range is applied to the biosensing system and the corresponding frequency signatures of the combinatorial biosensor in terms of impedance are recorded (Randviir and Banks, 2013). Typically, in biological systems non-faradaic EIS allows one to understand the surface and bulk phenomenon that occurs in a biosensing system when a biological buffer solution interacts with a charged electrode surface (Lisdat and Schäfer, 2008). We are interested in understanding the surface phenomenon that takes place at the hybrid electrode- solution interface which contributes to the impedance response of the combinatorial biosensor. The interaction of the buffer solution with the charged hybrid electrode results in the formation of an electrical double layer (EDL). The EDL of the hybrid electrode- solution interface is modeled as a Randles circuit [See Fig. S5]. Capacitive effects are more predominantly observed in non-faradaic EIS in the frequency regime < 1KHz. In enzyme systems, charge transfer process occurs due to the electron- transfer between the enzyme complex and the electrode surface but its effects are more pronounced in lower frequency regimes (Randviir and Banks, 2013) (Lisdat and Schäfer, 2008). Non- faradaic chronoamperometry is a DC based quantitative technique that captures currents from the non-faradaic processes occurring in the double layer as a function of time. In response to an applied DC pulse, the recorded current consists of a non- faradic current arising from the charging of the double layer, and a capacitive decay current caused by the relaxation of the double layer (Scholz, 2015).

3.2 AC and DC based performance evaluation and sensor calibration of the alcohol biosensor in synthetic sweat of varying pH's

The calibration of the biosensor's response to alcohol concentrations in SS of pH 4, 6, and 8 are represented as calibration dose response (CDR) curves in Fig. 2A, 2B, and 2C. The CDR curves are plotted as percentage change in impedance of the dose concentrations with respect to baseline in the sweat buffers. The impedance variations across a frequency range of 1Hz- 1MHz were analyzed. A high signal to noise ratio (SNR) was observed within the 10– 1KHz range at which the percentage change in impedance with respect to baseline was

maximum. However, we choose 100Hz as our calibration frequency to compare the responses of the two biomolecules of interest and for the ease of integration with portable electronics towards developing a point- of-care diagnostic device. As shown in Figs. 2A, 2B, and 2C the percentage change in impedance response from 0.01 to 100 mg/dl was observed to be ~20% in SS of pH 4 and 6 and ~30% in SS of pH 8. The SST for alcohol biosensing in SS buffers lies below the percentage impedance response of the lowest alcohol concentration being detected. It is observed that the LOD for the combinatorial biosensor in detecting alcohol in SS of varying pH's is 0.01 mg/dl. The dynamic range of alcohol detection is 0.01– 100 mg/dl. The pH of the buffer solution effects the charge behavior of ZnO and the stability of the enzymatic activity (Mohd Omar et al., 2014) (Azevedo et al., 2005). Change in impedance produced by the biosensor in response to the increasing target biomolecule concentrations is facilitated by a combination of two processes: (1) charge modulation occurring within the double layer (2) charge transfer occurring between the enzyme biomolecule complex when the target biomolecules.

The measured current of the chronoamperometric responses reflect the non-faradaic charge transfer between the enzyme complex and the capacitive current for the double layer. The calibration curves shown in Figs. 2D, 2E, and 2F are plotted for the average change in steady state current from the baseline obtained for varying alcohol concentrations. We observe that the current response decreases with increasing pH which corroborates with the increasing impedance observed with increasing pH in the EIS studies.

3.3 AC and DC based performance evaluation and sensor calibration of the alcohol biosensor in perspired human sweat

The calibration dose response curves obtained for alcohol biosensing in human sweat buffer (pH ~5.98) using EIS and CA are shown in Figs. 4A and 4C. The percentage change in impedance for logarithmic alcohol concentrations between 0.01– 100 mg/dl varies from 12– 35%. The LOD of the combinatorial biosensor for alcohol detection in human sweat is found to be 0.1 mg/dl with a dynamic range is 0.1– 100 mg/dl (Gamella et al., 2014). The sweat alcohol content for <1–3 drinks detected by the biosensor marked by the color bands in Fig. 4A lie well within the relevant range of alcohol found in human sweat. The LOD and the standard deviation is higher in human sweat as it as complex biomatrix consisting of interferents that contribute to the noise factor. The average current change from the baseline from the lowest to the highest alcohol concentration in the CDR is the 0.4(±0.17)- 2 (±0.8) μA. A correlation coefficient of $R^2 = 0.98$ is calculated for the CDRs obtained using EIS and CA. CA captures the temporal response of the biosensor as an average function of current change derived from the double layer relaxation, mobility of ions in the solution, and the time dependent electric field experienced by the ions (Bard and Faulkner, 2000). However, EIS is a powerful sensitive technique that allows characterization of biosensor system by detecting a time- based impedance response across a frequency spectrum. The impedance response is a summation of the individual responses obtained from the bulk solution resistance, charge transfer resistance, and the double layer capacitance. Due to the sensitivity of EIS in capturing the biomolecular events at the EDL interface as individual events rather than an average function, the LOD for alcohol detection in human sweat is one logarithmic concentration higher than the LOD detected by the chronoamperometric technique.

3.4   AC and DC based performance evaluation and sensor calibration of the glucose biosensor in synthetic sweat of varying pH's

The calibration of the combinatorial biosensor's response to glucose in sweat buffers of pH's 4, 6, and 8 are shown in Figs. 3A, 3B, and 3C. An increasing percentage change in impedance is observed with increasing logarithmic glucose concentrations from 0.01– 50 mg/dl spiked in SS of pH 4, 6, and 8. At pH 4, the percentage impedance change from the baseline was observed to be between 10– 40% from the lowest to the highest glucose concentration. The percentage changes in impedance in SS pH 6 for the increasing glucose concentrations varied from 16– 50%. Higher percentage changes in impedance between 22– 58% with a standard deviation of 5– 11% were observed in SS pH 8. The LOD in SS of pH's 4, 6, and 8 is found to be 0.01 mg/dl.

The chronoamperometric responses of the combinatorial biosensor in detecting glucose concentrations in SS of pH 4, 6, and 8 are shown in Figs. 3D, 3E, and 3F respectively. For SS pH 4, the average change in current produced by the increasing glucose concentrations from the baseline varies from 2.4 ($\pm$0.4) - 8.4 ($\pm$1.2) µA. The current changes observed for glucose concentrations from 0.01– 500mg/dl in synthetic sweat of pH 6 is 1.9 ($\pm$0.8) - 5.5 ($\pm$1) µA whereas in SS pH 8, the current changes in the range of 1.7($\pm$0.4) - 5.4 ($\pm$0.9) µA are observed for the lowest to the highest dose concentration. The LOD computed across synthetic buffers for CA based glucose detection is 0.01 mg/dl.

3.5   AC and DC based performance evaluation and sensor calibration of the glucose biosensor in perspired human sweat

The EIS- based performance of the combinatorial biosensor in detecting glucose in perspired human sweat represented by the calibration dose response curves are shown in Fig. 4B. The percentage change in impedance varies from 14– 35% for logarithmic glucose concentrations ranging from 0.01– 50 mg/dl. A correlation coefficient of $R^2 = 0.95$ is obtained after performing regression analysis. The LOD is found to be 0.1mg/dl and the dynamic range of glucose detection is 0.01– 50 mg/dl. The sweat glucose concentrations corresponding to hypoglycemic, normal, and hyperglycemic levels are marked by color bands in Figs. 4B. The larger deviations obtained at the elevated glucose concentrations could be induced by the steric hindrances from the size of glucose molecules and cross- talk from the sweat interferents [See section 3.6]. The deviations lie within 15% which meet the standards set by Clinical and Laboratory Standards Institute (CLSI)(Interference Testing in Clinical Chemistry; and Approved Guideline—Second Edition).

The chronoamperometric calibration dose response curve for glucose detection in human sweat as shown in Fig. 4D. The average change in current for the glucose range 0.01– 50 mg/dl varies from 2.3($\pm$0.7) - 4.8($\pm$0.6) µA. The current changes obtained from the non-specific biomolecules present in human sweat cannot be decoupled from the behavior obtained from the specific biomolecules hence affecting the linearity and the lower detection limit of the CDR. The LOD obtained is 0.01mg/dl. A correlation coefficient $R^2 = 0.82$ is obtained from the regression analysis.

3.6 Performance of the biosensors in the presence of cross- reactive biomolecules in synthetic sweat

The reliability of the combinatorial sensor in detecting specific target biomolecules of interest and no other molecules can been investigated from cross- reactivity analysis. The combinatorial biosensor relies on the functionalized enzyme-biomolecule complex to selectively oxidize specific biomolecules and to have minimal non- specific interactions. To assess the specificity of the alcohol and glucose immunoassays developed on the combinatorial biosensor, cross- reactivity studies were performed in SS pH 6 with alcohol and glucose as described in Section 2.5.

The impedance response of glucose as a cross- reactive biomolecule spiked in SS pH 6 on the alcohol sensor is shown in Fig. 5A. The median percentage changes in impedance increase linearly from 12.5– 31% with increasing logarithmic alcohol concentrations with a noise threshold of 11%. The impedance signals obtained from the cross- reactive glucose molecules vary between 2.5 –10% and lie below the noise threshold. The response of the glucose sensor to cross- reactive alcohol molecules spiked in SS pH 6, as shown in Fig. 5B, shows an increasing trend in median percentage change in impedance ranging from 22– 55% with logarithmic glucose concentrations. The variation in response from the alcohol molecules lies within the range 1– 7% and falls below the noise threshold of 14%. The linearly increasing impedance response obtained from the specific interactions and flat impedance trend obtained from the cross-reactive molecules indicate that the electrochemical signal response in obtained only from the specific interactions of biomolecules with their specific enzyme complexes. The combinatorial biosensor is feasible in distinguishing the non-specific interactions from the specific interactions.

3.7 Continuous combinatorial monitoring of alcohol in perspired human sweat

The robustness and stability of the combinatorial biosensor is evaluated by performing dynamic continuous monitoring of alcohol in perspired human sweat. The dynamic impedance response of the combinatorial biosensor to alcohol concentrations equivalent to consuming <1– 3 standard drinks i.e. 3– 125 mg/dl alcohol in perspired human sweat obtained at 100Hz is depicted in Figure 6A. The rate of change in impedance slopes as a function of drink dose are observed to be 1.7 Ω/min for <1 drink, 42.7 Ω/min for 1 drink, 113. 4 Ω/min for 2 drinks, and 269.8 Ω/min for 3 drinks. An incremental impedance response is observed with increasing alcohol dose concentrations over a 110-minute duration implying that the rate of change of impedance is entirely drink dependent. This time limited dynamic monitoring of alcohol in human sweat when extended to longer periods as desired in real -world applications, would indicate similar trends inimpedance response over time proportional to drink consumed. A correlation coefficient R^2 =0.99 is obtained from a polynomial curve fitted to the impedance response.

3.8 Continuous, dynamic monitoring of the effect of hypoglycemic and hyperglycemic glucose levels on perspired human sweat alcohol content

We have demonstrated for the first time in this paper, the dynamic interplay in the temporal variations of alcohol and glucose. The dynamic response of the alcohol biosensor is tested to understand the modulation in alcohol levels under the influence of hyperglycemic and

hypoglycemic glucose levels. The typical sweat glucose concentrations corresponding to hypoglycemic, normal, and hyperglycemic lie within the range 0.85– 5.5 mg/dl (Lee et al., 2016). A drink dependent increasing trend in impedance is observed proportional to the alcohol concentration consumed in the presence of hypoglycemic and hyperglycemic glucose levels as shown in Figs. 6C and 6D respectively. The rate of change in impedance slopes as a function of drink dose in the presence of hypoglycemic glucose levels are observed to be 0.05 KΩ/min for <1 drink, 0.52 KΩ/min for 1 drink, 0.9 KΩ/min for 2 drinks, and 1.2 KΩ/min for 3 drinks. The rate of change in impedance slopes as a function of drink dose in the presence of hyperglycemic glucose levels are observed to be 0.06 KΩ/min for <1 drink, 0.68 KΩ/min for 1 drink, 0.73 KΩ/min for 2 drinks, and 1.15 KΩ/min for 3 drinks. An R^2 value of 0.99 was obtained for both the polynomial fits.

3.9 Continuous, dynamic monitoring of perspired sweat glucose on consumption of <1–2 standard drinks

Continuous monitoring of glucose levels in diabetic individuals with a social drinking lifestyle is essential for diabetes management. Two scenarios representing the effect of evening consumption of alcohol on next morning glucose levels subject to nourishment states are illustrated in Fig. 1C. The temporal modulations in the glucose levels on drink consumption to simulate real-life situations to control drink consumption is evaluated on the glucose biosensor. The change in impedance response observed from the varying glucose levels – hypoglycemic (0.85mg/dl), normal (2mg/dl), hyperglycemic (5.5mg/dl) on consuming <1– 2 standard drinks in shown in Figs. 6E and 6F over a 120-minute duration. The rate of change of in the slope of impedance response is glucose level dependent. The rate of change in impedance slopes as a function of glucose concentrations in the presence of alcohol equivalent to <1 standard drink is observed to be 27.3 Ω/min for hypoglycemic level, 108.6 Ω/min for normal level, and 395.1 Ω/min for hyperglycemic level. The rate of change in impedance slopes as a function of glucose concentrations in the presence of alcohol equivalent to 2 standard drink is observed to be 40.6 Ω/min for hypoglycemic level, 185 Ω/min for normal level, and 769. 2 Ω/min for hyperglycemic level. Polynomial curve fit to the impedance responses for both cases yield an R^2 of 0.99.

Conclusion

This work is the first- time demonstration of a biosensor utilizing ultra- low passive perspired human sweat volumes for rapid and dynamic monitoring of alcohol and glucose in a temporal manner suitable for wearable IOT applications. A relationship between blood glucose levels and consumption of alcohol has been found to interfere with blood glucose levels and reduce the effectiveness of insulin (Emanuele et al., 1998) (Avogaro and Tiengo, 1993). Alcohol consumption is prone to increasing diabetes related risks leading to acute hypoglycemia or hyperglycemia depending on the body's nutrition state. To maintain a healthy wellness state, it is imperative to track the fluctuations caused in glucose levels and to limit one's alcohol intake through investigation of human bodily fluids. In this work, we have demonstrated the combinatorial detection of alcohol and glucose in human sweat using electrochemical impedance spectroscopy and CA as a comparative analysis technique. A thorough analysis of effects of pH of the sweat buffers on the combinatorial biosensor's

performance in detecting target biomolecules of interest yielded an outcome that the ionicity of buffer plays a key role in giving out reliable and stable sensor output. The biosensor enables users to track the interplay between glucose and alcohol in a "real- time" manner. Shift in linearity of the impedance response and differing LOD's obtained in human sweat are primarily due to the sensitivity of the detection techniques in deconvoluting the specific interactions between the target biomolecules – enzyme biomolecule complex and the non - specific interactions originating from the interferents present in human sweat buffer. Cross-reactivity studies revealed negative interactions from the cross-reactive biomolecules that lie well within the noise threshold of the biosensor. The combinatorial biosensor's performance in monitoring alcohol and glucose in perspired human sweat in continuous and dynamic manner has been demonstrated towards making it suitable for developing a wearable lifestyle monitor for limiting alcohol intake in the diabetic and prediabetic population. The dynamic effects exerted by a chronic cohort of alcohol and glucose molecules on each other are continuously monitored through their impedance responses which indicate an incremental rate of change in impedance response proportional to the biomolecule concentration levels. This work demonstrates a non- invasive, label- free approach towards translation onto portable diagnostic platforms for monitoring vital statistics through analysis of ultra- low volumes of passive perspired sweat.

Supplementary Material

Refer to Web version on PubMed Central for supplementary material.

Acknowledgements

References

1. Abrar MA , Dong Y , Lee PK , Kim WS , 2016 Scientific Reports. 6, 30565.27465437

2. Anastasova S , Crewther B , Bembnowicz P , Curto V , Ip HM , Rosa B , Yang GZ , 2017 Biosens. Bioelectron 93, 139–145.27743863

3. Armbruster DA , Pry T , 2008 The Clinical Biochemist Reviews. 29, S52.

4. Avogaro A , Tiengo A , 1993 Diabetes. Metab 9, 129–146.

5. Azevedo AM , Prazeres DMF , Cabral JMS , Fonseca LP , 2005 Biosensors and Bioelectronics. 21, 235–247.16023950

6. Babor T , Rehm J , Jernigan D , Vaeth P , Monteiro M , Lehman H , 2012 Revista panamericana de salud pública = Pan American journal of public health. 32, 151.23099877

7. Bard AJ , Faulkner LR , 2000 Electrochemical Methods: Fundamentals and Applications. Wiley.

8. Diabetes.org, 2017.

9. Du X , Anzai J , Osa T , Motohashi R , 1996 Electroanalysis. 8, 813–816.

10. Emanuele NV , Swade TF , Emanuele MA , 1998 Alcohol Health Res. World 22, 211–219.15706798

11. Evans D , 2011 The Internet of Things: How the Next Evolution of the Internet is Changing Everything.

12. Gamella M , Campuzano S , Manso J , Rivera GG , López-Colino F , Reviejo AJ , Pingarrón JM , 2014 Anal. Chim. Acta 806, 1–7.24331037

13. Gao W , Emaminejad S , Nyein HYY , Challa S , Chen K , Peck A , Fahad HM , Ota H , Shiraki H , Kiriya D , Lien D , Brooks GA , Davis RW , Javey A , 2016 Nature. 529, 509–514.26819044

14. Haghi M , Thurow K , Stoll R , 2017 Healthc. Inform. Res 23, 4–15.28261526

15. Interference Testing in Clinical Chemistry, Approved Guideline—Second Edition.

16. Jason H , 2016 Electroanalysis. 28, 1242–1249.

17. Jia W , Bandodkar AJ , Valdés-Ramírez G , Windmiller JR , Yang Z , Ramírez J , Chan G , Wang J , 2013 Anal. Chem 85, 6553–6560.23815621

18. Kim J , Jeerapan I , Imani S , Cho TN , Bandodkar A , Cinti S , Mercier PP , Wang J , 2016 ACS Sens. 1, 1011–1019.

19. Lee H , Choi TK , Lee YB , Cho HR , Ghaffari R , Wang L , Choi HJ , Chung TD , Lu N , Hyeon T , Choi SH , Kim D , 2016 Nature Nanotechnology. 11, 566.

20. Lisdat F , Schäfer D , 2008 Analytical and Bioanalytical Chemistry. 391, 1555.18414837

21. Mathew MT , Ariza E , Rocha LA , Fernandes AC , Vaz F , 2008 Tribology International. 41, 603–615.

22. Mohd Omar F , Abdul Aziz H , Stoll S , 2014 Science of The Total Environment. 468–469, 195–201.24742557

23. Moyer J , Wilson D , Finkelshtein I , Wong B , Potts R , 2012 Diabetes Technol. Ther 14, 398–402.22376082

24. Munje RD , Muthukumar S , Prasad S , 2017 Sensors and Actuators B: Chemical. 238, 482–490.

25. NIAAA, 2015.

26. Randviir EP , Banks CE , 2013 Anal. Methods 5, 1098–1115.

27. Hiremath S , Yang G , Mankodiya K , 2014 2014 4th International Conference on Wireless Mobile Communication and Healthcare - Transforming Healthcare Through Innovations in Mobile and Wireless Technologies (MOBIHEALTH), 304–307.

28. Scholz F , 2015 ChemTexts. 1, 17.

29. Swan M , 2012 Journal of Sensor and Actuator Networks. 1.

30. Thomas N , Lähdesmäki I , Parviz BA , 2012 Sensors Actuators B: Chem. 162, 128–134.

HIGHLIGHTS

- Combinatorial biosensor for continuous, dynamic monitoring of alcohol and glucose in ultra- low volumes of passive perspired sweat

- Biomolecular interactions occurring at the electrode- sweat interface in response to double layer charge modulations are evaluated using non-faradaic EIS and CA

- Detection of physiologically relevant ranges of alcohol (3 – 125mg/dl) and glucose (0.85 to 5.5mg/dl) in perspired human sweat

- Demonstration of stable temporal response on continuous exposure to alcohol and glucose in perspired human sweat over a 120-minute duration.
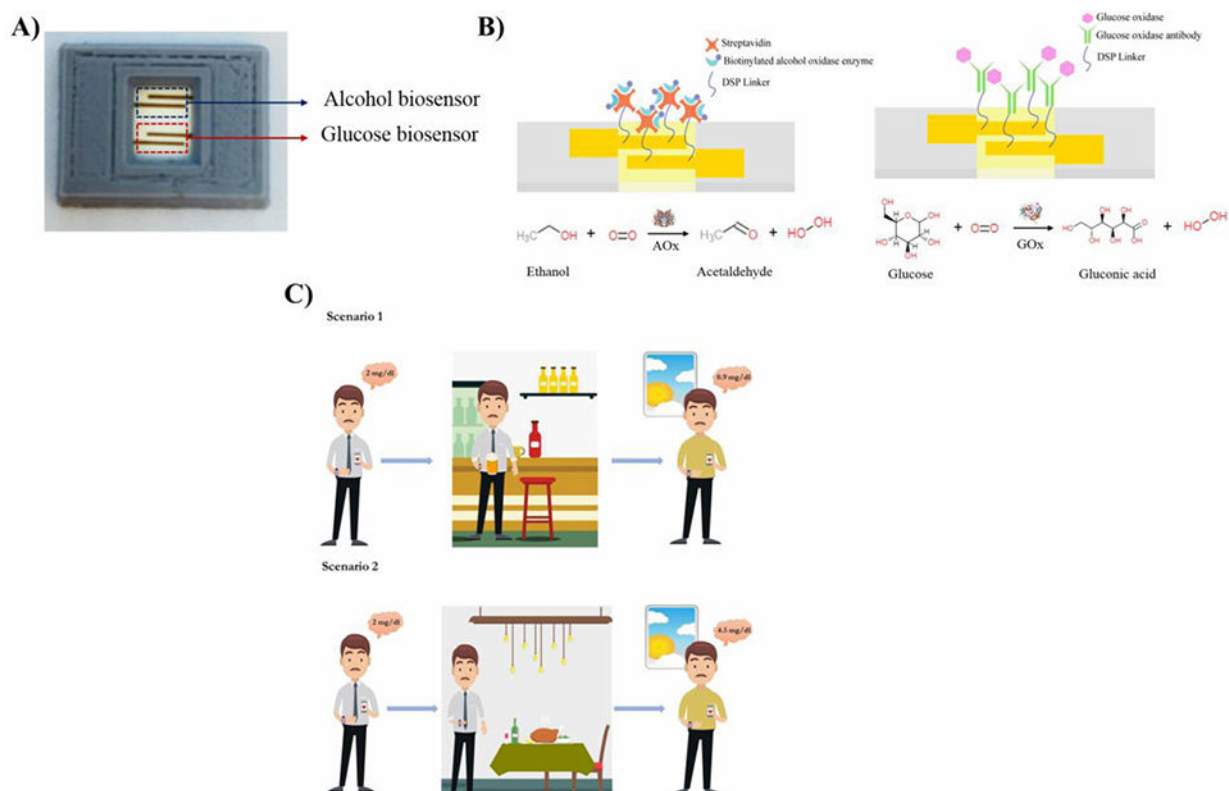
Fig 1.
(A) Picture of the combinatorial biosensor (B) Schematic of the functionalized immunoassays for the combinatorial detection of alcohol and glucose in synthetic sweat and perspired human sweat (C) Scenarios illustrating the relationship between evening alcohol consumption and next morning glucose levels in pre-diabetic and diabetic populations subject to their nourishment state.
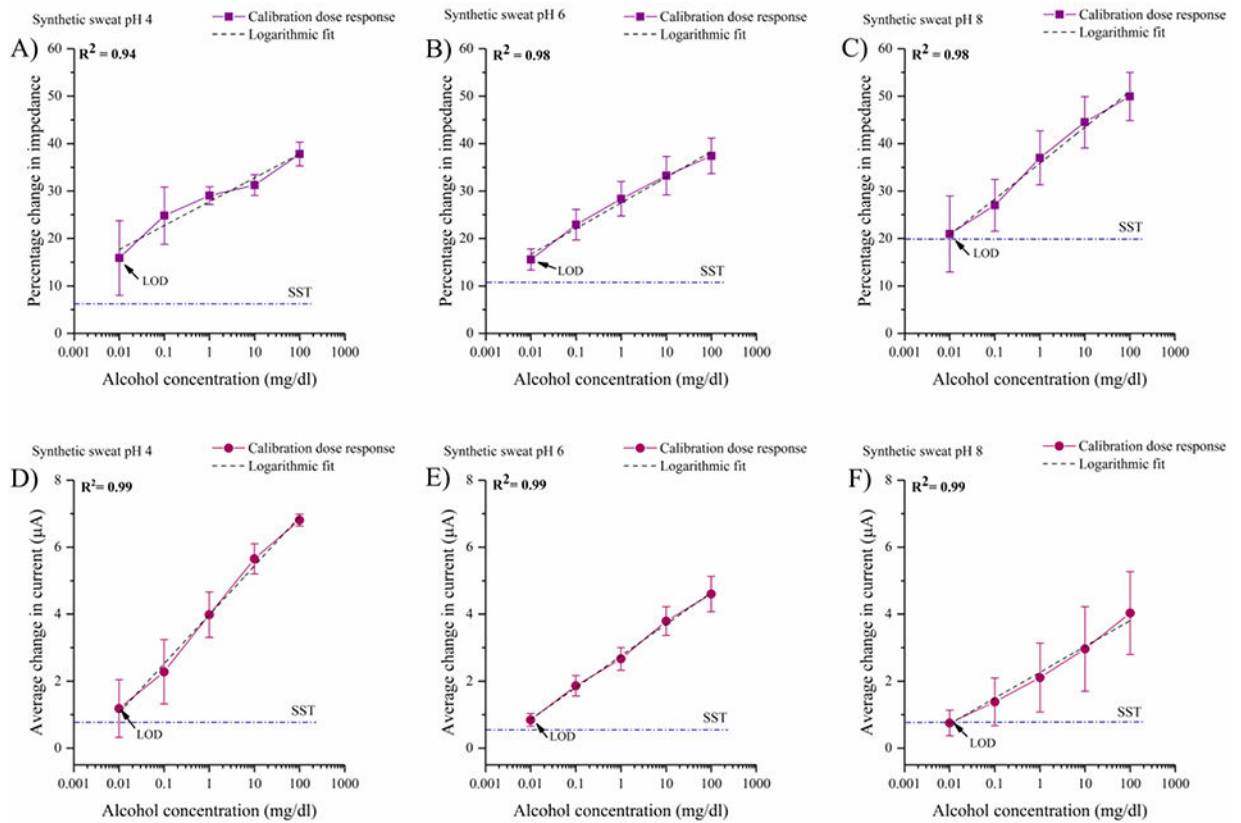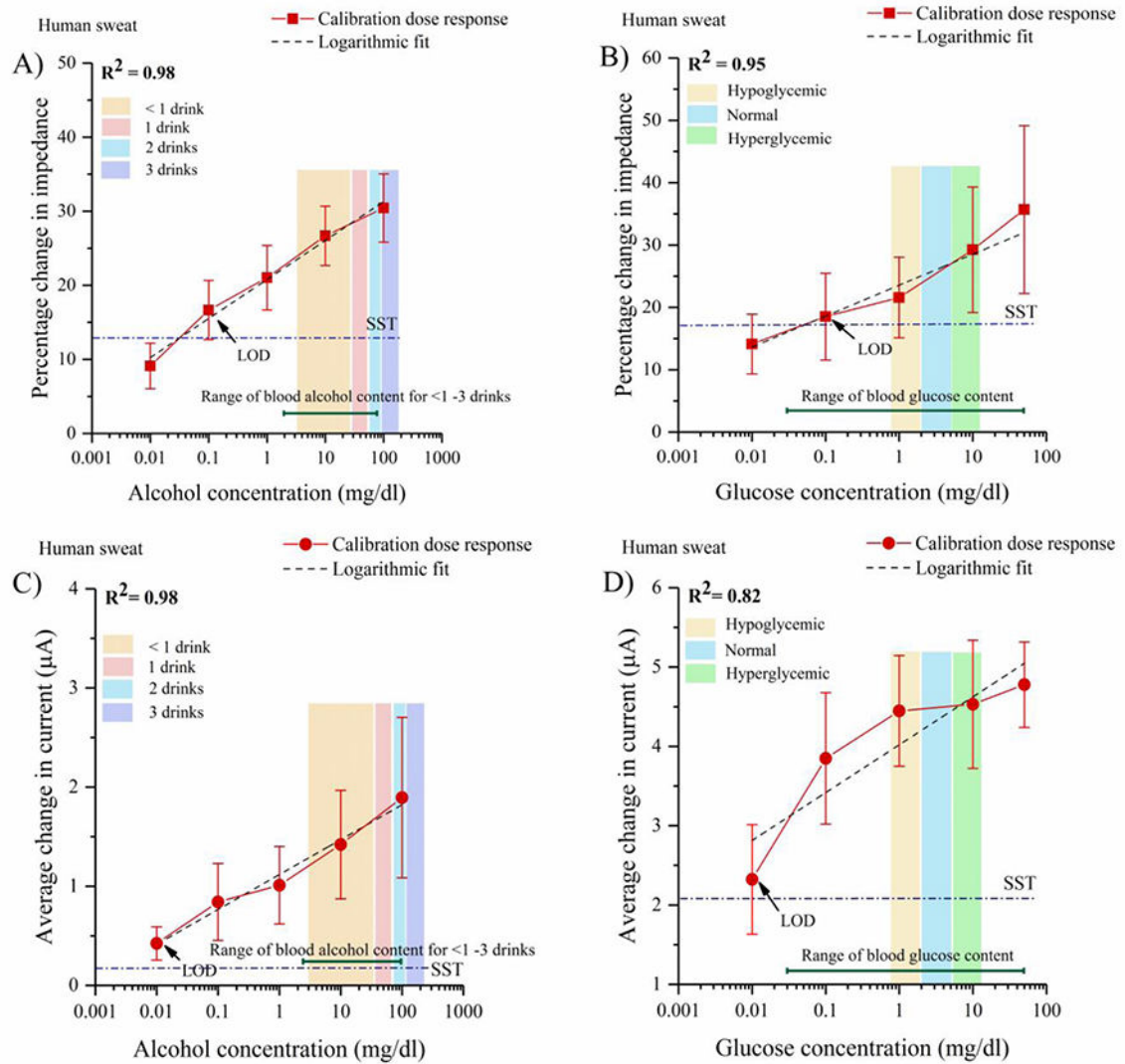
Fig 2.
Calibration dose response of alcohol as a function of percentage change in impedance at 100 Hz in (A) synthetic sweat buffer of pH 4 (B) synthetic sweat buffer of pH 6 (C) synthetic sweat buffer of pH 8. Calibration dose response chronoamperograms for alcohol as a function of average change in current from the baseline in (D) synthetic sweat buffer of pH 4 (E) synthetic sweat buffer of pH 6 (F) synthetic sweat buffer of pH 8
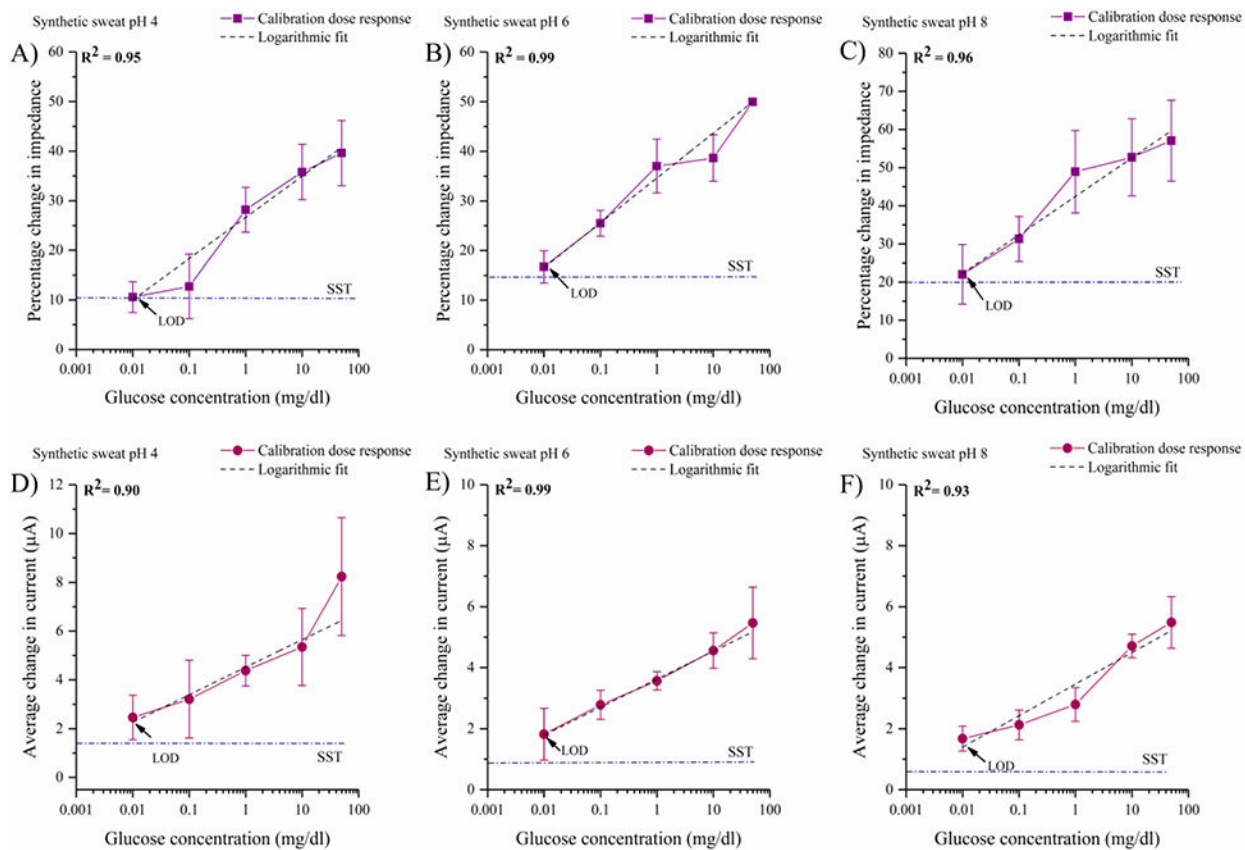
Fig 3.
Calibration dose response of glucose as a function of percentage change in impedance at 100 Hz in (A) synthetic sweat buffer of pH 4 (B) synthetic sweat buffer of pH 6 (C) synthetic sweat buffer of pH 8. Calibration dose response chronoamperograms for glucose as a function of average change in current from the baseline in (D) synthetic sweat buffer of pH 4 (E) synthetic sweat buffer of pH 6 (F) synthetic sweat buffer of pH 8

Fig 4.
(A) Calibration dose response of alcohol as a function of percentage change in impedance at 100 Hz in perspired human sweat (B) Calibration dose response of glucose as a function of percentage change in impedance at 100 Hz in human sweat (C) Calibration dose response chronoamperograms for alcohol as a function of average change in current from the baseline in perspired human sweat (D) Calibration dose response chronoamperograms for glucose as a function of average change in current from the baseline in human sweat
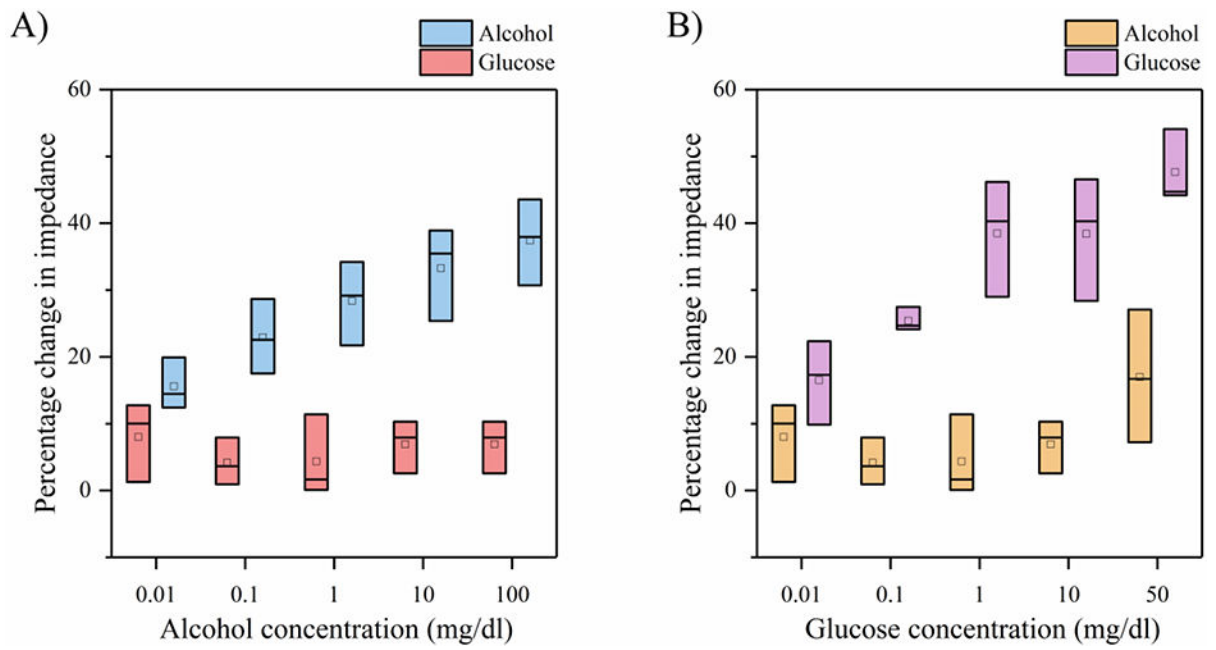
Fig 5.
(A) Alcohol biosensor selectivity for glucose as the cross- reactive molecule in synthetic sweat on pH 6 (B) Glucose biosensor selectivity for alcohol as the cross- reactive molecule in synthetic sweat on pH 6
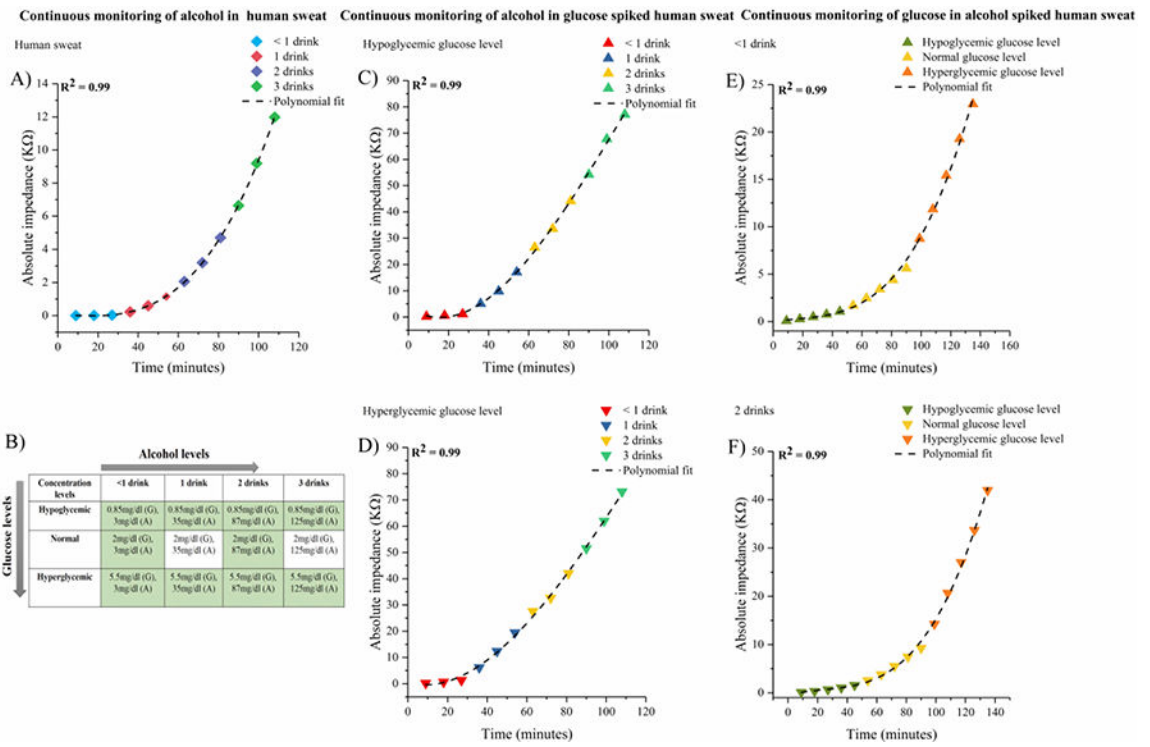
Fig 6.
(A) Continuous and dynamic monitoring of alcohol spiked in perspired human sweat. (B) Alcohol and glucose dose combination index for combinatorial biosensing. Continuous dynamic monitoring of alcohol in (C) hypoglycemic glucose spiked perspired human sweat (D) hyperglycemic glucose spiked perspired human sweat. Continuous dynamic monitoring of glucose in (E) alcohol equivalent to <1 drink spiked perspired human sweat (F) alcohol equivalent to 2 drinks spiked perspired human sweat